Research Square

Preprints are preliminary reports that have not undergone peer review.
They should not be considered conclusive, used to inform clinical practice,
or referenced by the media as validated information.

LRCH4 drives tumor cell proliferation by regulating the GSK3B/MEK/ERK axis in colorectal cancer

Zhengyu Wu
Guizhou Medical University
Juan Wang
Guizhou Moutai Hospital
Wei Zhan
The Affiliated Hospital of Guizhou Medical University
Ling Li
Guizhou Medical University
Xuanzhen Qian
Guizhou Medical University
Bi Wang
wangbi@gmc.edu.cn
Guizhou Medical University
Rui Li
Beijing Jishuitan Hospital Guizhou Hospital

Research Article

Keywords: colorectal cancer, LRCH4, GSK3B, MEK/ERK axis, proliferation, biomarker, therapeutic target

Posted Date: June 5th, 2026

DOI: https://doi.org/10.21203/rs.3.rs-9448013/v1

License: This work is licensed under a Creative Commons Attribution 4.0 International License.
Read Full License

Additional Declarations: No competing interests reported.

Abstract

Leucine-rich repeat-containing protein 4 (LRCH4), a member of the LRCH family, has emerged as a potential prognostic biomarker in several cancers, including colorectal cancer (CRC). While other proteins in this family have been implicated in tumorigenesis, the specific role of LRCH4 in CRC remains poorly understood. This study aimed to elucidate the clinical significance and biological function of LRCH4 in CRC. Bioinformatics analysis of The Cancer Genome Atlas data revealed that LRCH4 was significantly upregulated in CRC tissues, and its high expression correlated with poor patient prognosis. Gene set enrichment analysis suggested its potential involvement in the Kirsten Rat Sarcoma Viral Oncogene Homolog (KRAS) signaling pathway. Using mass spectrometry and co-immunoprecipitation assays, we identified glycogen synthase kinase 3B (GSK3B) as a novel binding partner of LRCH4. Functional experiments demonstrated that LRCH4 binds to GSK3B and inhibits its phosphorylation, thereby activating downstream MEK/ERK signaling to promote cell proliferation. An in vivo xenograft model confirmed that the knockdown of LRCH4 expression suppressed tumor growth. Furthermore, immunohistochemical analysis of clinical samples validated the negative correlation between high LRCH4 expression and patient survival rate. In conclusion, our findings establish LRCH4 as a key oncoprotein that drives CRC proliferation by directly modulating the GSK3B pathway, highlighting its potential as both a prognostic biomarker and a promising therapeutic target.

Introduction

Colorectal cancer (CRC) is the third most commonly diagnosed malignancy and the second leading cause of cancer-related death globally, following lung cancer [1]. Despite advances in early detection and therapeutic strategies that have contributed to declining mortality rates, clinical outcomes remain suboptimal due to high rates of recurrence and metastasis [2]. A primary factor underlying this poor prognosis is the current lack of robust, reliable biomarkers for early diagnosis and effective targeted therapies [3,4]. Consequently, elucidating the molecular mechanisms that drive CRC progression and identifying novel, high-fidelity biomarkers are critical imperatives for improving diagnostic accuracy, prognostic stratification, and therapeutic efficacy.

Leucine-rich repeat-containing protein 4 (LRCH4) is a member of the LRCH family, which plays crucial roles in immune activation and the maintenance of body homeostasis [5]. A key functional domain of LRCH4 is its transmembrane (TM) region, which is essential for binding lipopolysaccharides (LPS) at the cell membrane [6]. It is worth noting that the mortality rate of acute myeloid leukemia (AML) patients with elevated LRCH4 levels is significantly reduced [7]. Research using the Cancer Genome Atlas (TCGA) database has shown that the expression of LRCH4 varies significantly at different stages (I-IV) of cancer, and it is one of the genes most closely associated with adverse outcomes in CRC patients [8]. Although previous studies have shown that knockdown of LRCH4 inhibits the proliferation, migration, and invasion of HT-29 cells—a well-established human colorectal adenocarcinoma cell line—by affecting extracellular matrix (ECM) remodeling, epithelial-mesenchymal transition (EMT), and YAP and TGF-β/Smad signaling

pathways [9], the precise downstream partners of LRCH4 and their physiological functions in vivo remain incompletely understood.

The RAS-RAF-MEK-ERK signaling cascade is critical for regulating cell growth, survival, and differentiation, and its dysregulation is a key driver in various cancers [10]. RAS gene mutations Kirsten Rat Sarcoma Viral Oncogene Homolog (KRAS) occur in about 20% of human cancers with a tissue-specific pattern: KRAS mutations dominate in gastrointestinal and lung cancers (e.g., 90% of pancreatic, 50% of colorectal, 25% of lung adenocarcinomas), NRAS mutations in melanoma (~ 20%) and hematologic malignancies, and HRAS mutations in urinary, endocrine, and head and neck cancers [11]. KRAS mutations alter the tumor immune microenvironment to promote immune escape through multiple mechanisms, such as by activating the MEK-ERK-p38-MK2 pathway and inhibiting the TTP-mediated degradation of PD-L1, thereby stabilizing PD-L1 levels [12–13]. Therefore, a comprehensive understanding of RAS-related signaling molecules and pathways, both upstream and downstream, remains essential in oncology research.

In this study, we found that LRCH4 expression was significantly upregulated in CRC tissues compared to matched normal tissues. This elevated expression was associated with enhanced cell proliferation and poor patient prognosis. To investigate the underlying mechanism, we employed co-immunoprecipitation coupled with mass spectrometry, in vitro cellular assays, xenograft tumor models, and clinical sample analysis. Our results demonstrate that LRCH4 promotes CRC growth by interacting with glycogen synthase kinase 3B (GSK3B) and activating the downstream MEK pathway. These findings suggest that LRCH4 could serve as a valuable biomarker for the diagnosis and prognosis of CRC.

Material and Methods

2.1. Data Processing

The expression profiles of 33 distinct tumor types were analyzed, as cataloged by the TCGA (https://www.cancer.gov/ccg/research/genomesequencing/tcga) initiative. It is important to note that this research adhered to the guidelines outlined by TCGA, which resulted in the waiver of ethical approval and the need for informed consent from the patients involved.

2.2. KEGG pathway and GO term enrichment

KEGG pathway and GO term enrichment was acquired using the online DAVID enrichment analysis service. Enrichment was considered significant following Benjamini–Hochberg multiple comparison adjustment with a FDR threshold of < 0.05. Gene Set Enrichment Analysis (GSEA) was performed using the "clusterProfiler" package (version 3.17.0) to conduct set enrichment analysis. The analysis utilized the Hallmark MSigDB gene sets as the reference gene sets for the enrichment process.

2.3. Clinical specimens

A total of six patients diagnosed with colon adenocarcinoma were prospectively enrolled in this study (3 male and 3 female; median age: 65 years; age range: 50–80 years). Patient recruitment and sample collection occurred between January 2023 and December 2024. The inclusion and exclusion criteria were as follows: no neoadjuvant chemotherapy, radiotherapy, or immunotherapy prior to surgery. For each patient, matched tissue samples—including histologically confirmed normal colonic mucosa, peritumoral tissue, and primary tumor tissue—were collected during surgical resection. Normal tissue, peritumoral tissue, and tumor tissue were all obtained from the same patient. The tissue samples for this experiment were collected from CRC patients at the Affiliated Hospital of Guizhou Medical University. All participants provided written informed consent prior to enrollment, explicitly authorizing the use of their tissue specimens exclusively for non-commercial, academic research purposes, and this study was approved by the hospital's Medical Ethics Committee.

2.4. Prognostic Analysis

The relevant data information comes from a published clinical study related to the clinical outcomes of CRC patients [14], including overall survival, progression-free interval, and disease-specific survival. Kaplan-Meier survival analysis was used to analyze the correlation between LRCH4 and GSK3B expression and the prognosis of CRC patients.

2.5. Western Blot

Cells were lysed in RIPA buffer (P0013B, Beyotime, Shanghai, China) containing a protease inhibitor cocktail (4693132001, Roche, Shanghai, China). Protein analysis was performed using the BCA assay kit (P0009, Beyotime Institute of Biotechnology). After protein separation by SDS-PAGE, the embedded proteins were transferred to a PVDF membrane (ISEQ00010, EMD Millipore, Shanghai, China). The membrane was then blocked with 5% non-fat milk in TBS buffer at room temperature (RT) for 2 hours and incubated overnight with the following primary antibodies: anti-LRCH4 (1:1000, TQ-KLS-18978, TechiSun), anti-GSK3B (1:1000, 22104-1-AP, Proteintech), anti-P-GSK3B (Tyr216) (1:1000, 29125-1-AP, Proteintech), anti-MEK (1:1000, 11049-1-AP, Proteintech), anti-P-MEK (1:1000, 9121S, Cell Signaling Technology), anti-ERK (1:1000, 11257-1-AP, Proteintech), anti-P-ERK (1:1000, 28733-1-AP, Proteintech), and anti-GAPDH (1:1000, 60004-1-Ig, Proteintech). The membranes were incubated with HRP conjugated Affinipure Goat anti Mouse (1:2000, SA-00001-1, Proteintech) or HRPconjugated Affinipure Goat anti Rabbit secondary antibodies (1:2000, SA-00001-2, Proteintech) at room temperature for 1 hour after three washes with TBST, followed by imaging using the LI-COR Odyssey®CLx imaging system.

2.6. immunohistochemistry (IHC) assay

Paired tumor and adjacent specimens were collected from patients diagnosed with colon cancer. Four-millimeter-thick sections were stained with anti-LRCH4, anti-P-GSK3B (Tyr216), and Ki-67 antibodies. Immunoreactivity scoring was used to quantify IHC staining results. Positive staining percentage scores were as follows: 1 (10%), 2 (10–50%), 3 (50–75%), and 4 (> 75%). Intensity was defined as 0–3: 0, no staining; 1, weak staining; 2, moderate staining; 3, strong staining. The staining index is obtained by

multiplying these two scores. In the analysis, scores of 8–12 are considered high expression, and scores of 0–6 are considered low expression.

2.7. Cell lines and antibodies

HCT-116 cells were cultured in McCOY's 5A medium supplemented with 10% foetal bovine serum, LOVO cells were cultured in F-12K medium supplemented with 10% foetal bovine serum, 293(T) cells were cultured in Dulbecco's Modified Eagle Medium supplemented with 10% foetal bovine serum. All three cell lines were cultured at 37°C and 5% CO_2.

2.8. Quantitative real-time PCR

Total RNA extraction for real-time fluorescent quantitative PCR was performed using TRIzol™ reagent (Invitrogen, Shanghai, China) according to the manufacturer's instructions. Total RNA quantification was performed using Nanodrop, and cDNA synthesis was performed using the HiScript II First Chain cDNA Synthesis Kit (Vazyme, Nanjing, China) according to the manufacturer's protocol. cDNA was amplified using 2x Universal SYBR Green Fast qPCR Mix (abClon, Wuhan, China) on the StepOne™ Applied Biosystems real-time fluorescent quantitative PCR system. Primer sequences were as follows: β-Actin, forward 5’ -gggaaatcgtgcgtgacattaag, reverse 5’ -tgtgttggcgtacaggtctttg; LRCH4, forward 5’ -gtctgcctgaaggggaaact, reverse 5’ -cttgctgccactatcaacgc. Relative changes in expression levels were calculated using the formula fold change = $2^{-\Delta\Delta ct}$ [15]. All measurements were performed in at least triplicate, and experiments were conducted independently at least three times.

2.9. Cell transfection and inhibitors

Plasmids overexpressing LRCH4 (LRCH4-ov/Flag-LRCH4), GSK3B (GSK3B-ov/Myc-GSK3B), and an empty vector were purchased from Miaoling (Wuhan, China). For transient transfection, cells were transfected with the indicated plasmids using Lipofectamine 8000 reagent (Cat#: C0533, Beyotime) according to the manufacturer's instructions. Cells were collected 24 hours after transfection. LRCH4 expression was inhibited in HCT-116 and LOVO cells using an LRCH4 shRNA strategy. The following sequences were used: shLRCH4#1 (5’caccgcttcaagcgccggttagac-3’), shLRCH4#2 (5’caccgcagtacgctgcccgaagag-3’), shGSK3B#1 (5’caccgcgactgttccccattcgcc-3’), shGSK3B#2 (5’caccgtctgcggtttaatatcccg-3’), shNC(5’tcctaaggttaagtcgccctc3’). 293(T) cells were used to package lentiviral vectors expressing LRCH4 shRNA, GSK3B shRNA, or control shRNA. Seed HCT-116 and LOVO cells into six-well culture plates. The culture medium was replaced with lentiviral particles for 24 hours, and after 2 days, cells were selected for stable integration using 1–3 μg/ml puromycin (Sigma-Aldrich, St. Louis, MO, USA). The stable clones were picked and the expression of LRCH4 and GS3KB was examined by western blot.

2.10. Immunoprecipitation (IP) assays

Cells were lysed in ice-cold RIPA solution for 30 minutes and then centrifuged. The supernatant was mixed with 20 μl of blank magnetic beads (#HY-K0202, MCE, NJ, USA) for 2 h. Subsequently, 3–5 μl of antibody was added to 40 μl of magnetic beads, and the mixture was resuspended in 500 μl of RIPA lysis

buffer. The mixture was incubated overnight at 4°C. The magnetic beads were separated from the mixture and incubated with the protein supernatant at 4°C. After 4 h, the samples were boiled with SDS loading buffer and collected for subsequent experiments.

2.11 Mass spectrometry

The IP-enriched LRCH4 protein samples and blank control IgG samples were digested, dried, and redissolved in 0.1% trifluoroacetic acid. The peptides were analyzed using an Orbitrap fusion mass spectrometer.

2.12. Cell Counting Kit-8 (CCK8) and 5-Ethyl-2-Deoxyuridine (EdU) Assay

HCT-116 and LOVO cells transfected with shNC, shLRCH4#1, and shLRCH4#2 were seeded into 96-well plates (5 × 10^3 cells/well). After 48 hours, 10 μL of CCK8 solution was added to each well. After incubation for 2 hours, absorbance was measured at 450 nm using a microplate reader. To measure cell proliferation capacity, the EdU assay was performed according to the manufacturer's protocol. Images were observed under a fluorescence microscope.

2.13. Colony Formation

Treated HCT-116 and LOVO cells were cultured in 6-well plates (1,000 cells/well) for 2 weeks. Clones were stained with crystal violet, and ImageJ software (V.1.52a; NIH, New York, NY, USA) was used to quantify the colonies.

2.14. Mouse tumor xenograft model

Male BALB/c nude mice aged 4 to 6 weeks (18 ± 5 g) were provided by Beijing Huafukang Biotechnology Co., Ltd. and housed under specific pathogen-free conditions. HCT-116 cells or LOVO cells stably expressing shNC, shLRCH4#1, and shLRCH4#2 (5 × 10^6 cells per mouse, resuspended in 100 μL matrigel) were subcutaneously injected into the right inguinal region of BALB/c nude mice (n = 5 per group) [16–17]. Tumor growth was monitored every 5 days for 25 days, and tumor volume was measured using calipers and calculated as (length × $width^2$)/2. Animal health and behavior, including activity, food and water intake, body weight changes, tumor appearance, and signs of distress or abnormal behavior, were monitored daily throughout the experiment. Humane endpoints were established as follows: tumor volume exceeding 1000 mm^3, tumor ulceration or infection, body weight loss exceeding 20% of initial body weight, or significant impairment of mobility or moribund state. Animals reaching any of these endpoints would be immediately euthanized. In this study, no animals reached the humane endpoints prior to the end of the experiment. After 25 days, all mice were euthanized by cervical dislocation; no unexpected deaths occurred during the experiment. Tumors were excised, weighed, photographed, and their volumes measured. All tumors were paraffin-embedded, sectioned, and subjected to immunohistochemical staining, followed by microscopic examination. Animal experiments were approved by the Animal Care and Use Committee of Guizhou Medical University.

2.15. Statistical analysis

All data were processed using GraphPad Prism 9.0 software. Data are shown as mean ± SEM. Unpaired two-tailed t-tests were used for between-group comparisons (*P < 0.05; **P < 0.01; ***P < 0.001; ****P < 0.0001). For multiple-group comparisons, one-way ANOVA was first applied, followed by Tukey's post hoc test to pinpoint specific differences.

Results

3.1. LRCH4 is upregulated in colorectal cancer and associated with poor prognosis.

Analysis of LRCH4 mRNA expression using TCGA data across 33 cancer types revealed significant upregulation in 10 malignancies (Fig. 1A). Notably, none of the cancer types assessed exhibited a significant decrease in LRCH4 expression. Specifically, in CRC, LRCH4 expression was markedly elevated in tumor tissues compared with adjacent non-tumor tissues in both paired and unpaired analyzes (Fig. 1B-C). These findings were validated in our clinical cohort of 12 paired CRC samples, where qPCR confirmed significantly higher LRCH4 mRNA levels in tumors than in matched normal tissues (Fig. 1D). Consistent with mRNA data, western blot analyzes further demonstrated pronounced upregulation of LRCH4 protein in CRC specimens (Fig. 1E). Clinically, Kaplan–Meier survival analysis indicated that high LRCH4 expression was significantly associated with unfavorable outcomes, including shorter overall survival, disease-specific survival, and progression-free interval (Fig. 1F-H). Taken together, these data identify LRCH4 as an overexpressed gene in CRC that correlates with aggressive disease and poor prognosis.

3.2. LRCH4 promotes colorectal cancer cell proliferation.

To investigate the role of LRCH4 in CRC cell proliferation, we established stable knockdown and overexpression models in two distinct CRC cell lines. Western blot analysis confirmed successful LRCH4 overexpression and effective protein reduction with two specific shRNAs (Fig. 2A). CCK-8 assays demonstrated that LRCH4 overexpression significantly enhanced cell viability, whereas LRCH4 knockdown substantially suppressed this activity (Fig. 2B). The results of cell cloning experiments showed that knockdown of LRCH4 expression significantly inhibited cell proliferation (Fig. 2C-D). Consistent with these findings, EdU incorporation assays also showed that knockdown of LRCH4 significantly reduced DNA synthesis ability, while overexpression of LRCH4 significantly enhanced cell proliferation activity (Fig. 2E-F). In summary, these results provide compelling evidence that LRCH4 plays a crucial role in promoting the growth of CRC cells.

3.3. LRCH4 binds GSK3B and potentiates MEK/ERK signaling in colorectal cancer.

To elucidate the mechanism by which LRCH4 promotes CRC cell proliferation, we first performed bioinformatic analysis using the DAVID database with Gene Ontology (GO) and Kyoto Encyclopedia of Genes and Genomes (KEGG) pathway enrichment. KEGG analysis revealed significant enrichment in biological processes related to chromatin organization and DNA replication assembly (Fig. 3A). Subsequent Gene Set Enrichment Analysis indicated potential activation of the KRAS signaling pathway upon LRCH4 upregulation (Fig. 3B). To identify direct interacting partners of LRCH4, we transfected 293(T) cells with Flag-LRCH4 or control plasmid and performed co-immunoprecipitation (co-IP) with anti-Flag antibody, followed by mass spectrometry analysis. This screening identified GSK3B as a prominent binding partner of LRCH4 (Fig. 3C). The interaction was further confirmed by co-IP assays in 293(T) cells co-transfected with Flag-LRCH4 and Myc-GSK3B (Fig. 3D). Additionally, endogenous co-IP experiments using antibodies against LRCH4 or GSK3B validated their physiological interaction in native cellular contexts (Fig. 3E). Previous studies have shown that the phosphorylation status of GSK3B plays a crucial role in controlling tumor cell proliferation through the classical Ras Raf MEK ERK signaling pathway. Our results indicate that overexpression of LRCH4 inhibits phosphorylation of GSK3B (Tyr216) and significantly increases phosphorylation of its downstream targets MEK and ERK. Knockdown of LRCH4 promotes phosphorylation of GSK3B (Tyr216) and inhibits phosphorylation of MEK and ERK (Fig. 3F). These results indicate that LRCH4 interacts with GSK3B to inhibit its phosphorylation, suggesting that LRCH4 may play a role in the proliferation of CRC through the GSK3B-mediated KRAS signaling pathway.

3.4. LRCH4 acts as an upstream regulator of GSK3B to drive oncogenic signaling

Next, we will further elaborate on the upstream and downstream relationship between LRCH4 and GSK3B. Overexpression of LRCH4 levels leads to significant inhibition of GSK3B (Tyr216) phosphorylation and enhanced downstream MEK and ERK phosphorylation. When LRCH4 and GSK3B were overexpressed, the phosphate levels of MEK and ERK returned to their original state (Fig. 4A). However, overexpression and knockdown of GSK3B had no effect on the expression level of LRCH4 (Fig. 4B). This indicates that the inhibitory effect of LRCH4 on this signaling pathway is mediated by GSK3B. We further evaluated the role of GSK3B in LRCH4-mediated tumor cell proliferation through CCK-8 and clone formation experiments. The results were consistent with Western blot results, showing that overexpression of LRCH4 significantly enhanced cell proliferation ability. However, overexpression of GSK3B at the same time did not result in any difference in cell proliferation activity compared to the control group (Fig. 4C-D). The above results further confirm the functional relationship between LRCH4 and GSK3B in regulating this signaling pathway. LRCH4 participates in downstream pathway regulation by regulating the phosphorylation of GSK3B (Tyr216).

3.5. LRCH4 promotes tumor growth in vivo by inhibiting GSK3B phosphorylation and correlates with poor patient survival

In order to confirm our results at the organizational level, in vivo experiments were conducted using a xenograft tumor model. On the 25th day after inoculation with CRC cells, euthanize the mice and collect the tumors. The xenografts of cells expressing shLRCH4 were significantly smaller, lighter, and paler, and the tumor growth curve also showed that compared with the control group, the growth rate of cells expressing shLRCH4 was significantly slower (Fig. 5A-B). In addition, IHC examination of mouse xenograft tumors showed that silencing of LRCH4 led to a significant increase in P-GSK3B (Tyr216) expression (Fig. 5C-F). Meanwhile, we also evaluated the expression of P-GSK3B (Tyr216) in samples from CRC patients using immunohistochemistry. The results showed that compared with adjacent non-tumor tissues and normal tissues, the expression of LRCH4 was significantly increased in tumor tissues, and the level of P-GSK3B (Tyr216) was significantly decreased (Fig. 6A-B). This is similar to the immunohistochemical results of xenograft tumor mouse tissue. In addition, the Kaplan Meier method was used to analyze the survival data. The reduced expression of GSK3B was significantly correlated with disease-specific survival and progression-free interval in patients with colorectal cancer (Fig. 6C-E). In summary, LRCH4 mainly participates in the subsequent activation of the MEK/ERK signaling pathway by regulating the phosphorylation of GSK3B (Tyr216), and plays a role in tumor cell proliferation.

Discussion

Although LRCH4 is known to regulate multiple signaling pathways influencing tumor growth, its precise molecular mechanisms and interacting partners are not fully understood. Here, by combining public database analysis with studies on paired clinical tissues, cell cultures, and animal models, we identified GSK3B activation as a key mechanism through which LRCH4 expression drives tumor proliferation. Mechanistically, LRCH4 binds to and inhibits the phosphorylation of GSK3B (Tyr216), which in turn activates the downstream MEK/ERK signaling cascade to drive tumor growth. These results suggest that both LRCH4 expression and GSK3B(Tyr216) phosphorylation status represent promising therapeutic targets and prognostic indicators in CRC.

LRCH proteins are classified as a new set of regulatory factors for the cytoskeleton [18]. Research has shown that LRCH4 inhibits immune inflammatory processes [19,20]. Previous bioinformatics analyses have suggested that LRCH4 may serve as a potential biomarker for several malignancies, such as CRC and AML [21]. It is worth noting that patients with elevated levels of LRCH4 in AML have significantly reduced mortality rates. We found that LRCH4 was overexpressed at both mRNA and protein levels in the collected tumor samples from cancer patients, which is consistent with the results of TCGA, and high expression of LRCH4 is significantly correlated with the survival rate of CRC patients. Potential mechanistic studies suggest that the absence of LRCH4 disrupts the YAP and TGF-β/Smad signaling pathways, reverses EMT, and alters the levels of ECM proteins, including fibronectin and type IV collagen [9]. In our study, we utilized two distinct colorectal cancer cell lines, HCT-116 and LOVO, which possess different genetic backgrounds and biological behaviors, to provide a comprehensive understanding of the role of LRCH4 in colorectal cancer. The results were consistent with previous findings, confirming that LRCH4 knockout reduces cell proliferation in vitro. Furthermore, this research demonstrates that LRCH4 promotes cell proliferation primarily through its interaction with GSK3B, thereby inhibiting

downstream pathways. We have confirmed the tumor suppressive effect of LRCH4 knockdown in vivo through a xenograft tumor model, providing stronger evidence for the role of LRCH4 in the progression of CRC.

GSK3B is a central signaling node in colorectal cancer, regulating cell proliferation by modulating β-catenin stability [22]. Under physiological conditions, GSK3B phosphorylates β-catenin, targeting it for degradation and thereby suppressing pro-proliferative gene expression [23,24]. In CRC, pathway dysregulation disrupts this phosphorylation, leading to β-catenin nuclear accumulation and activation of genes such as c-Myc, which promotes tumor development [25]. KRAS signaling further modulates GSK3B activity indirectly via downstream effectors like ERK and PI3K; for instance, KRAS-activated ERK can phosphorylate GSK3B, reducing its kinase activity, stabilizing β-catenin, and enhancing Wnt/β-catenin signaling—a mechanism that intensifies oncogenic signals in KRAS-mutant CRC [26–28]. Our results are consistent with this mechanistic framework, demonstrating that LRCH4 interacts with GSK3B to inhibit its phosphorylation, thereby leading to activation of the downstream MEK/ERK pathway. These findings establish LRCH4 as a key regulator of CRC progression via GSK3B-dependent signaling.

GSK3B activity is tightly regulated through site-specific phosphorylation at two key residues with opposing effects: phosphorylation at Ser9 (catalyzed by AKT/PKA) suppresses its kinase activity, while phosphorylation at Tyr216 within the activation loop enhances it [29]. While most colorectal cancer studies have traditionally evaluated GSK3B inactivation by measuring p-Ser9 levels [30,31], our investigation took a distinct approach by focusing on its active state through examination of p-Tyr216. We discovered that LRCH4 functions as a negative regulator of GSK3B activity. Specifically, in HCT-116 and LOVO CRC cell lines, LRCH4 binds to GSK3B and inhibits Tyr216 phosphorylation, maintaining GSK3B in a low-activity state. This, in turn, sustains MEK/ERK signaling, thereby promoting CRC cell proliferation. These findings underscore the precise control exerted by LRCH4 over GSK3B(Tyr216) phosphorylation within the tumor microenvironment, suggesting that in our model systems, LRCH4 exerts its oncogenic effects by suppressing the active form of GSK3B. Furthermore, we confirmed that LRCH4 is significantly overexpressed in CRC tissues, and its elevated levels are positively correlated with adverse clinical outcomes, underscoring its potential as a diagnostic and prognostic biomarker.

Nonetheless, this study still has limitations. Firstly, the changes in the active site Tyr216 of GSK3B were examined, while the potential involvement of its inhibitory phosphorylation at Ser9 in the regulation by LRCH4 was not investigated. Though p-Tyr216 can reflect kinase activity changes, future studies including p-Ser9 detection will better reveal LRCH4's overall impact on GSK3B's regulatory network. Secondly, although we have confirmed that LRCH4 drives colon cancer cell proliferation by regulating the GSK3B/MEK/ERK axis, this study did not conduct formal rescue experiments using GSK3B inhibitors or MEK inhibitors. Such experiments will further consolidate the conclusion that LRCH4 effect specificity is mediated by this cascade reaction and provide important directions for future research.

In summary, our research identifies LRCH4 as a key promoter of CRC growth in cellular and animal models. Mechanistically, LRCH4 directly binds to GSK3B, inhibiting its phosphorylation at the Tyr216 site,

thereby relieving the inhibition of the downstream MEK/ERK pathway and promoting tumor cell proliferation. (Fig. 7). These results imply that the levels of LRCH4 and the phosphorylation state of GSK3B may represent valuable targets for therapy and indicators for prognosis in CRC. Future studies should focus on elucidating the precise structural basis of the LRCH4-GSK3B interaction and evaluating the therapeutic potential of targeting this axis to impede CRC progression.

Abbreviations

CRC, Colorectal cancer; LRCH4, Leucine-rich repeat-containing protein 4; TCGA, The Cancer Genome Atlas; GSEA, Gene Set Enrichment Analysis; Glycogen synthase kinase-3 beta, GSK3B; KRAS, Kirsten Rat Sarcoma Viral Oncogene Homolog.

Declarations

Acknowledgments:

We would like to express our sincere gratitude to President Zhongzhu Chen, Dean Dianyong Tang, and Professor Kepeng Ou of Chongqing University of Arts and Sciences; as well as Director Rui Gao and Professor Xiao Zhou of the Guizhou International Travel and Medical Center. Their strong support and assistance played a crucial role in the successful completion of this project. Under the guidance of experts and their selfless dedication, this project was able to proceed smoothly.

Funding Information

This work was supported by the National Natural Science Foundation of China (82060523, 82160351) and the 2025 Annual Research Project of Guizhou Moutai Hospital

(MTyk2025-39).

Consent to publish

Written informed consent was obtained from the patient for publication of this article and any accompanying images. A copy of the written consent is available for review by the Editor-in-Chief of this journal.

Data availability

The datasets used and/or analyzed during the current study are available from the corresponding author on reasonable request.

Authors' contributions

ZY.W, J.W, L. L, XZ.Q: Data curation, Investigation, Methodology, Validation, Visualization, Writing - original draft. R.L, B.W, W.Z: Conceptualization, Formal analysis, Funding acquisition, Methodology,

Project administration, Resources, Supervision, Writing - review & editing. All authors reviewed the manuscript.

Ethics approval and consent to participate

The research protocol was approved by an Institutional Review Board. All human participants provided signed informed consent, and the study was conducted in accordance with the ethical standards of the institutional research committee and with the Helsinki Declaration. Formal approval was granted by the hospital's Medical Ethics Committee (ethics approval no. 2020052). All animal studies were conducted in compliance with institutional guidelines and were approved by the Animal Care and Use Committee of Guizhou Medical University (ethics approval no. 2100923).

Patient consent for publication

All patients provided written informed consent for the collection, storage, and research use of biological samples and associated clinical data, including anonymized data publication. This study was approved by the Medical Ethics Committee of Guizhou Medical University (Ethics approval No. 2020052).

Competing interests

The authors declare that they have no conflict of interest.

References

1. Biller LH and Schrag D. Diagnosis and Treatment of Metastatic Colorectal Cancer: A Review. JAMA. 2021;325:669-685.
2. Bray F, Laversanne M, Sung HYA, et al. Global cancer statistics 2022: GLOBOCAN estimates of incidence and mortality worldwide for 36 cancers in 185 countries. CA Cancer J Clin. 2024;74:229-263.
3. Miller KD, Nogueira L, Devasia T, et al. Cancer treatment and survivorship statistics, 2022. CA Cancer J Clin. 2022;72:409-436.
4. Lin DG, Fan WH, Zhang RX, et al. Molecular subtype identification and prognosis stratification by a metabolism-related gene expression signature in colorectal cancer. J Transl Med. 2021;19:279.
5. Rivière T, Bader A, Pogoda K, Walzog B, Maier-Begandt D. Structure and Emerging Functions of LRCH Proteins in Leukocyte Biology. Front Cell Dev Biol. 2020;8: 584134.
6. Aloor JJ, Azzam KM, Guardiola JJ, et al. Leucine-rich repeats and calponin homology containing 4 (Lrch4) regulates the innate immune response. J Biol Chem. 2019;294:1997-2008.
7. Sha K, Lu Y, Zhang P, et al. Identifying a novel 5-gene signature predicting clinical outcomes in AML. Clin Transl Oncol. 2021;23: 648-656.
8. Huo TY, Canepa R, Sura A, Modave F, Gong Y. Colorectal cancer stages transcriptome analysis. PLoS One. 2017;12:e0188697.

9. Li ZW, Cui ZH, Wang XR, Lv YF. Knockdown of LRCH4 Remodels Tumor Microenvironment Through Inhibiting YAP and TGF-β/Smad Signaling Pathway in Colorectal Cancer. Comb Chem High Throughput Screen. 2024;27:823-1829.
10. Hobbs GA, Der CJ, Rossman K. RAS isoforms and mutations in cancer at a glance. J Cell Sci. 2016;129:1287-92.
11. Prior IA, Hood FE, Hartley JL. The Frequency of Ras Mutations in Cancer. Cancer Res. 2020;80:2969-2974.
12. Punekar SR, Velcheti V, Neel BG, Wong KK. The current state of the art and future trends in RAS-targeted cancer therapies. Nat Rev Clin Oncol. 2022;19:637-655.
13. André, F, Arnedos, M, Baras, et al. AACR Project GENIE: Powering Precision Medicine through an International Consortium. Cancer Discov. 2017;7:818-831.
14. Liu JF, Lichtenberg T, Hoadley KA, et al. An Integrated TCGA Pan-Cancer Clinical Data Resource to Drive High-Quality Survival Outcome Analytics. Cell. 2018;173:400-416.
15. Livak KJ, Schmittgen TD. Analysis of relative gene expression data using real-time quantitative PCR and the $2^{-\Delta\Delta CT}$ method. METHODS. 2001;25:402-408.
16. Stribbling SM, Ryan AJ. The cell-line-derived subcutaneous tumor model in preclinical cancer research. Nat Protoc. 2022;17:2108-2128.
17. Yang YS, Liu CY, Wen D, et al. Recent advances in the development of transplanted colorectal cancer mouse models. Transl Res. 2022;249:128-143.
18. Sjöblom B, Ylänne J, Djinovic-Carugo K. Novel structural insights into F-actin-binding and novel functions of calponin homology domains. Curr Opin Struct Biol. 2008;18:702-8.
19. Dai K, Chen ZB, She S, Shi JZ, Zhu JL, Huang YB. Leucine rich repeats and calponin homology domain containing 1 inhibits NK-92 cell cytotoxicity through attenuating Src signaling. Immunobiology. 2020;225:151934.
20. Liu C, Xu XY, Han L, et al. LRCH1 deficiency enhances LAT signalosome formation and CD8(+) T cell responses against tumors and pathogens. Proc Natl Acad Sci USA. 2020;117:19388-19398.
21. Uhlen M, Zhang C, Lee S, et al. A pathology atlas of the human cancer transcriptome. Science. 2017;6352:eaan2507.
22. Wu H, Lu XX, Wang JR, et al. TRAF6 inhibits colorectal cancer metastasis through regulating selective autophagic CTNNB1/β-catenin degradation and is targeted for GSK3B/GSK3B-mediated phosphorylation and degradation. Autophagy. 2019;15:1506-1522.
23. Yan YR, Zhao PP, Wang ZH, et al. PRMT5 regulates colorectal cancer cell growth and EMT via EGFR/Akt/GSK3B signaling cascades. Aging (Albany NY). 2021;13:4468-4481.
24. Zeng X, Huang H, Tamai K, et al. Initiation of Wnt signaling: control of Wnt coreceptor Lrp6 phosphorylation/activation via frizzled, dishevelled and axin functions. Development. 2008;135:367-75.

25. Jia YA, Huang XY, Shi HY, et al. ADAMDEC1 induces EMT and promotes colorectal cancer cells metastasis by enhancing Wnt/β-catenin signaling via negative modulation of GSK-3B. Exp Cell Res. 2023;429:113629.
26. Krauss D, Moreno-Viedma V, Adachi-Fernandez E, et al. EGFR controls transcriptional and metabolic rewiring in KRASG12D colorectal cancer. EMBO Mol Med. 2025;17:1355-1392.
27. Eng, G and Yilmaz, O H. Plasticity as Resistance: KRAS Inhibition Reveals WNT Adaptation in Metastatic Colorectal Cancer. Cancer Discov. 2026;16:201-203.
28. Lea V, Lim SHS, Lee CS. Oncogenic mutations of clinical significance in colorectal cancer. Pathology. 2025;57:555-563.
29. Lochhead P, Kinstrie R, Sibbet G, Rawjee T, Morrice N , Cleghon V. A Chaperone-Dependent GSK3β Transitional Intermediate Mediates Activation-Loop Autophosphorylation. Mol Cell. 2006;24:627-33.
30. Feng Y, Xia YY, Yu G, et al. Cleavage of GSK-3β by calpain counteracts the inhibitory effect of Ser9 phosphorylation on GSK-3β activity induced by H_2O_2. J Neurochem. 2013; 126:234-42.
31. Xu XY, Zou L, Yao QH, et al. Silencing DEK downregulates cervical cancer tumorigenesis and metastasis via the DEK/p-Ser9-GSK-3β/ p-Tyr216-GSK-3β/β-catenin axis. Oncol Rep. 2017;38:1035-1042.

Figures

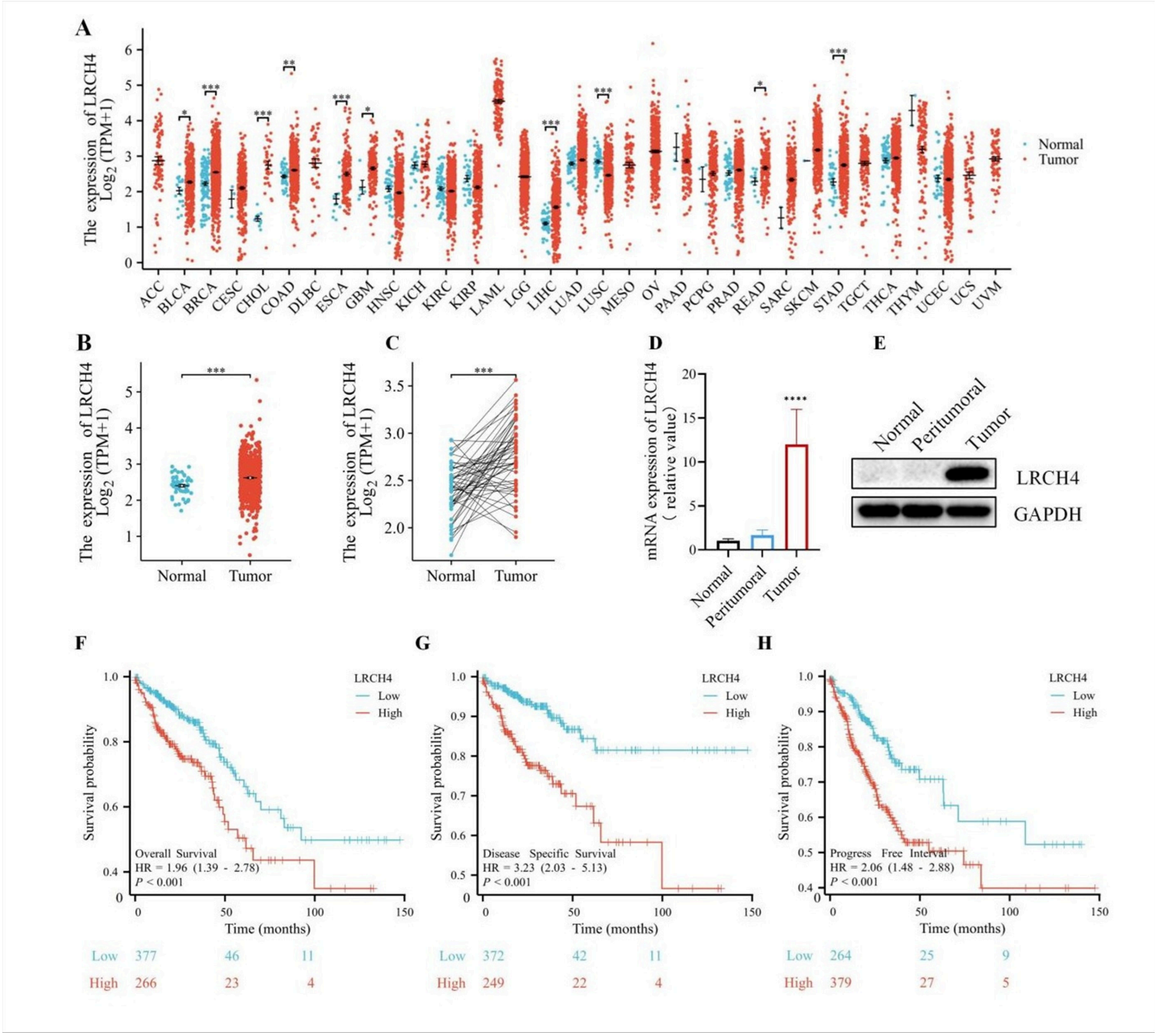


Figure 1

LRCH4 is upregulated in colorectal cancer and associated with poor prognosis. (A) LRCH4 mRNA levels across 33 types of tumors and corresponding normal tissues from TCGA database. Statistical significance is indicated as *p < 0.001, p < 0.01, *p < 0.05. (B, C) LRCH4 expression was significantly higher in CRC tumors compared to matched adjacent normal tissues in both (B) paired and (C) unpaired sample groups from the TCGA-CRC cohort (*p < 0.001). (D) qPCR validation of LRCH4 mRNA expression in 20 paired clinical CRC samples. Data are presented as mean ± SEM; **p < 0.0001. (E) Representative Western blot analysis of LRCH4 protein expression in normal, adjacent, and tumor tissues from CRC patients. (F-H) Kaplan-Meier survival curves for (F) overall survival (OS), (G) disease-specific survival

(DSS), and (H) progression-free survival (PFS) in CRC patients stratified by high vs. low LRCH4 expression. Data from TCGA dataset.

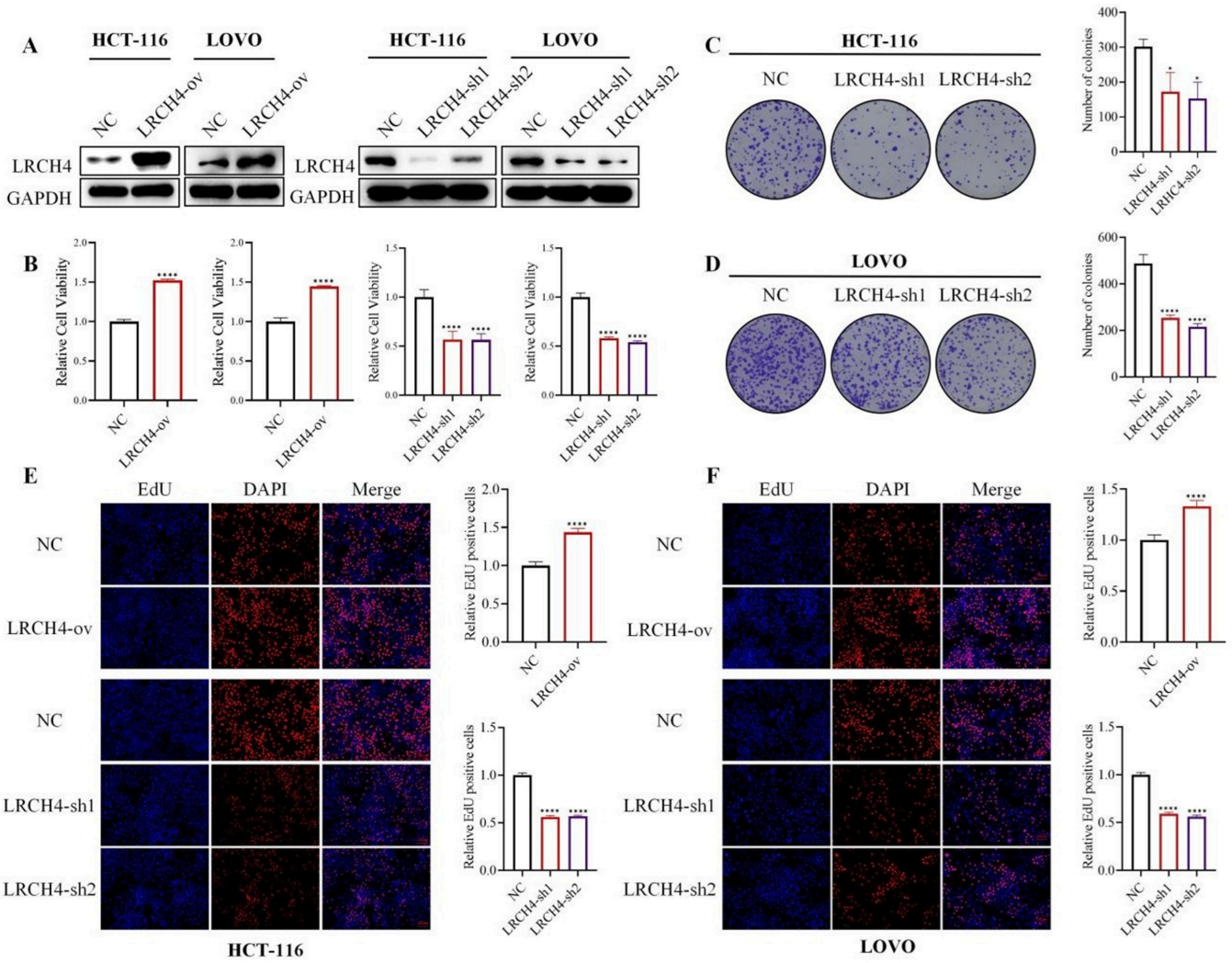


Figure 2

LRCH4 promotes the proliferation of colorectal cancer cells. (A) Western blot analysis of LRCH4 protein expression in HCT-116and LOVO cells following transfection with shLRCH4 or LRCH4-overexpression (LRCH4-OE) plasmids. (B) Cell viability was assessed by CCK-8 assay in HCT-116and LOVO cells with LRCH4 knockdown or overexpression. Data are presented as mean ± SEM; ****p < 0.0001. (C, D) Colony formation ability of HCT-116and LOVO cells in the negative control (NC), LRCH4-sh1, and LRCH4-sh2 groups. Representative images (C) and quantitative analysis of relative colony numbers (D) are shown. Data are presented as mean ± SEM; *p < 0.05, ****p < 0.0001. (E, F) DNA synthesis was evaluated by EdU assay. Representative images (E) and the percentage of EdU-positive cells (F) in HCT-116and LOVO cells with LRCH4 knockdown or overexpression are shown. Data are presented as mean ± SEM; ****p < 0.0001.

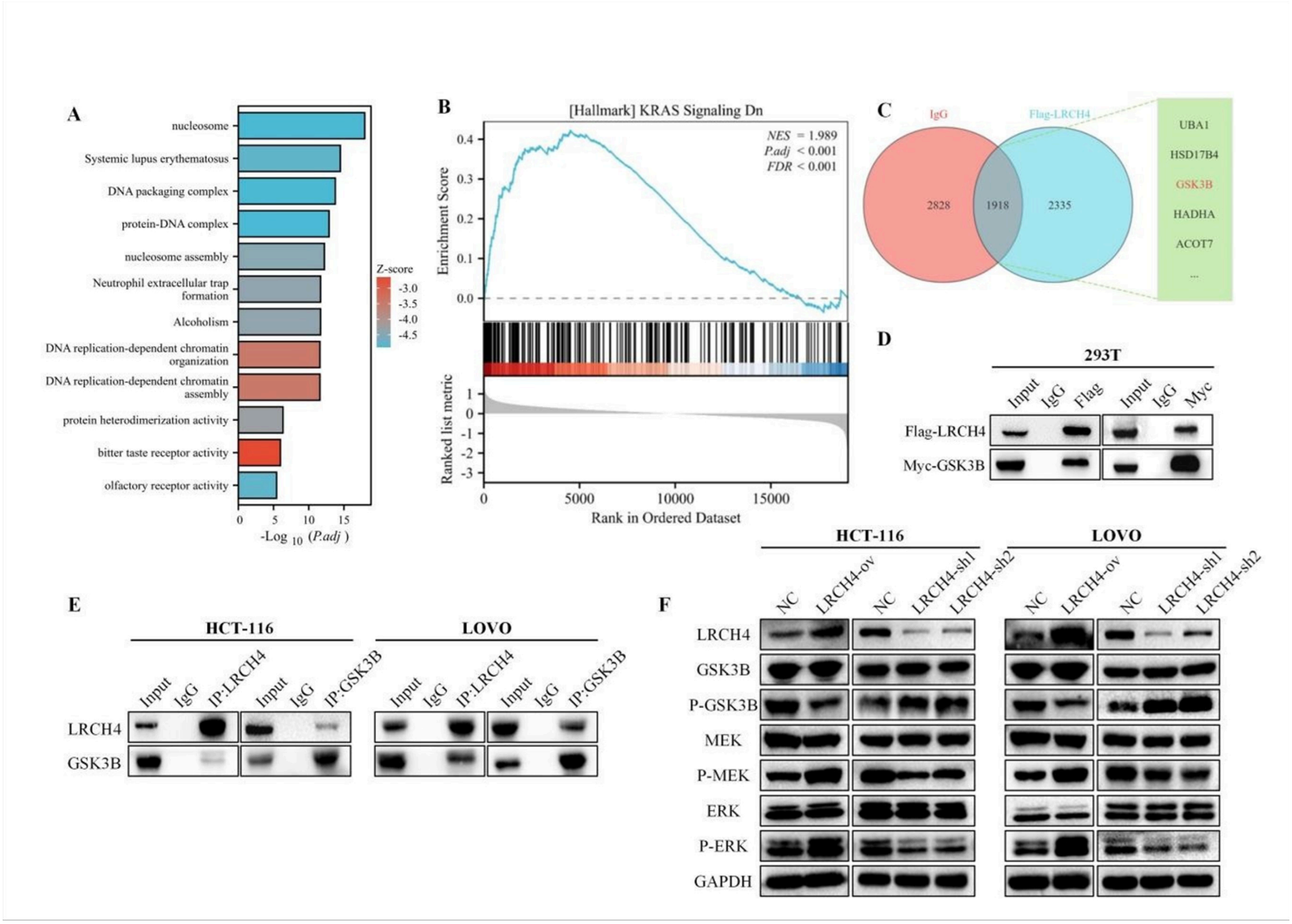


Figure 3

LRCH4 binds GSK3B and activates the MEK/ERK signaling pathway in colorectal cancer. (A) Gene Ontology (GO) enrichment analysis of LRCH4-associated genes in CRC, performed using the DAVID database, showing significantly enriched terms in biological process (BP), cellular component (CC), and molecular function (MF) categories. (B) Gene Set Enrichment Analysis reveals that LRCH4-associated differentially expressed genes are significantly enriched in the KRAS signaling pathway. (C) Venn diagram of potential LRCH4-interacting proteins identified by mass spectrometry. (D) Co-immunoprecipitation (Co-IP) assay confirming the interaction between overexpressed Flag-tagged LRCH4 and Myc-tagged GSK3Bin 293(T) cells. (E) Endogenous Co-IP assay validating the LRCH4-GSK3Binteraction in CRC cell lines (HCT-116and LOVO). (F) Western blot analysis of key KRAS pathway protein expression levels in control, LRCH4-knockdown, and LRCH4-overexpressing HCT-116and LOVO cells.

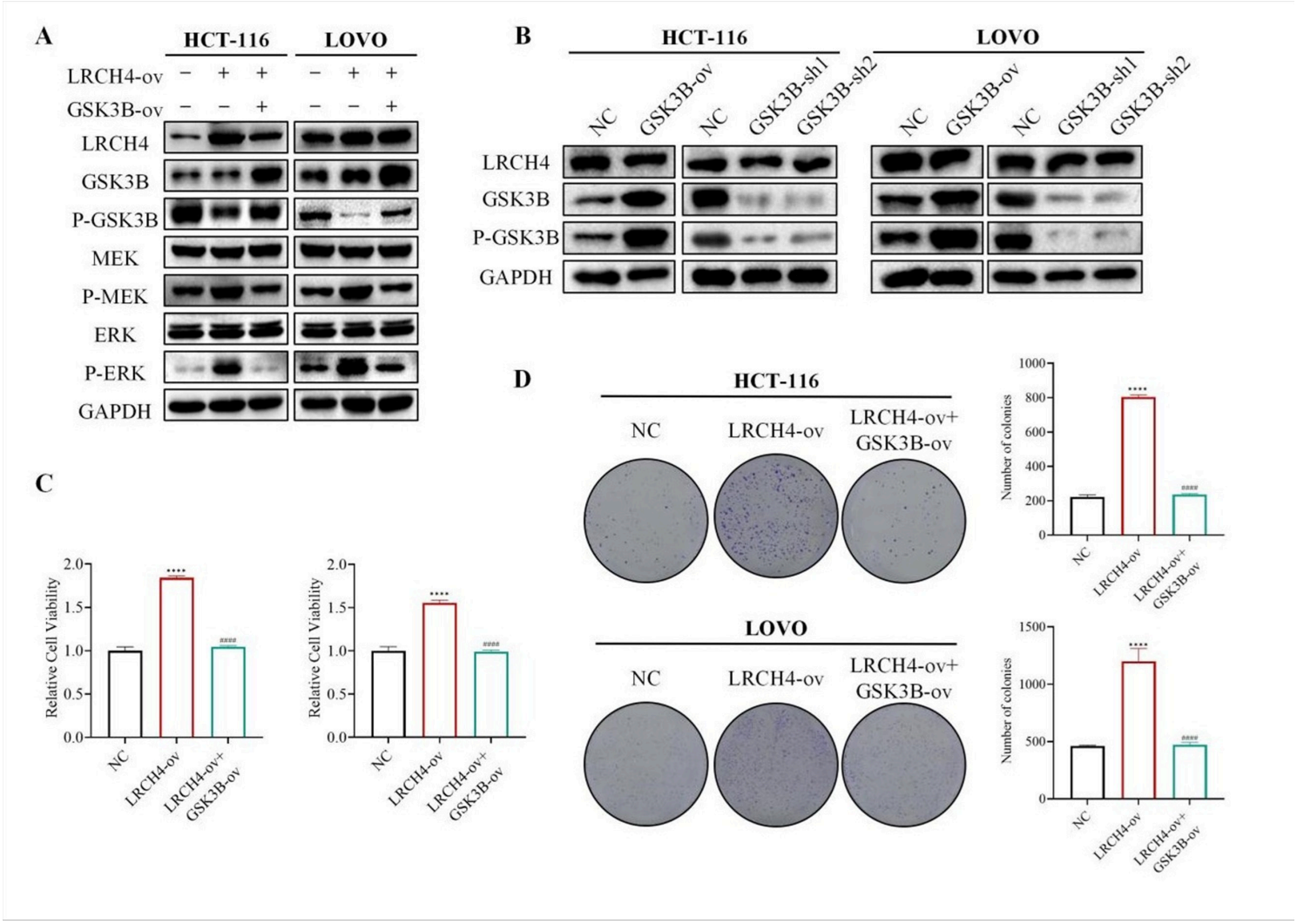


Figure 4

LRCH4 modulates KRAS-related pathways through GSK3B. (A) Western blot analysis of LRCH4, GSK3B, P-GSK3B, MEK, p-MEK, ERK, and p-ERK expression in HCT-116 and LOVO cells transfected with negative control (NC), LRCH4-overexpression (LRCH4-OE), or LRCH4-OE + GSK3B-OE constructs. (B) Western blot analysis of LRCH4, GSK3B, and P-GSK3B protein levels in HCT-116 and LOVO cells from the indicated groups: NC vs. GSK3B-OE (left), and NC vs. GSK3B-sh1 vs. GSK3B-sh2 (right). (C) Cell viability measured by CCK-8 assay in HCT-116 and LOVO cells from the NC, LRCH4-OE, and LRCH4-OE + GSK3B-OE groups. Data are presented as mean ± SEM; ****$p < 0.0001$ vs. NC group; $^{\#\#\#\#}p < 0.0001$ vs. LRCH4-OE group. (D) Colony formation assay in HCT-116 and LOVO cells from the NC, LRCH4-OE, and LRCH4-OE + GSK3B-OE groups. Representative images (left) and quantitative analysis of colony numbers (right) are shown. Data are presented as mean ± SEM; ****$p < 0.0001$ vs. NC group; $^{\#\#\#\#}p < 0.0001$ vs. LRCH4-OE group.

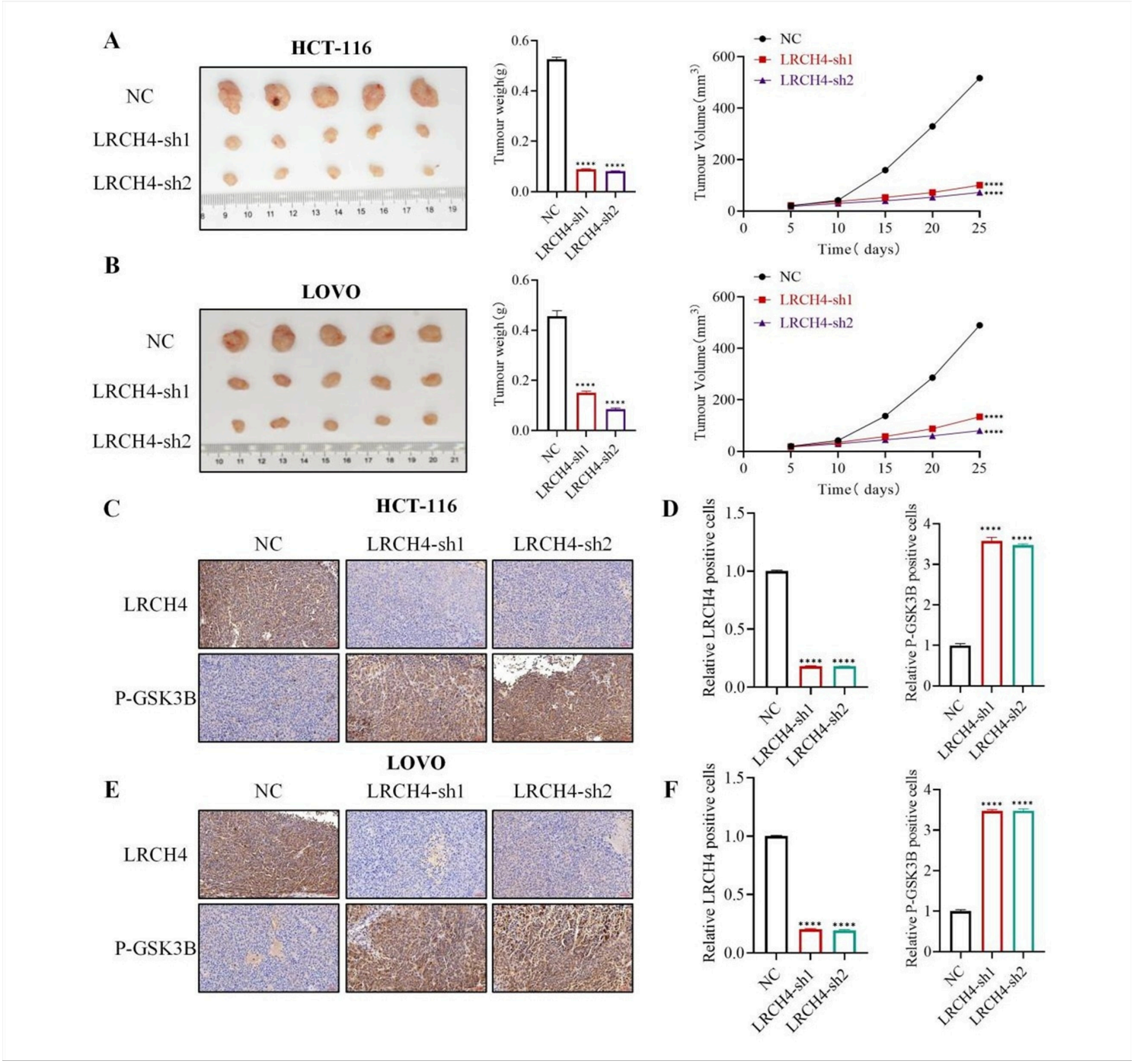


Figure 5

LRCH4 promotes tumor growth in vivo. (A, B) Xenograft tumor formation assay in nude mice injected with HCT-116(A) and LOVO (B) cells stably transfected with negative control (NC), shLRCH4-1, or shLRCH4-2 (n=5 per group). Left: Representative photographs of resected tumors at the endpoint (day 25). Middle: Comparison of final tumor weights. Right: Tumor growth curves measured over 25 days. Data are presented as mean ± SEM; ****p < 0.0001. (C-F) Representative IHC staining images of LRCH4 and P-GSK3Bin xenograft tumors of HCT-116and LOVO cells from different groups, and quantitative analysis of IHC staining. Staining intensity was scored and is presented as mean ± SEM; ****p < 0.0001.

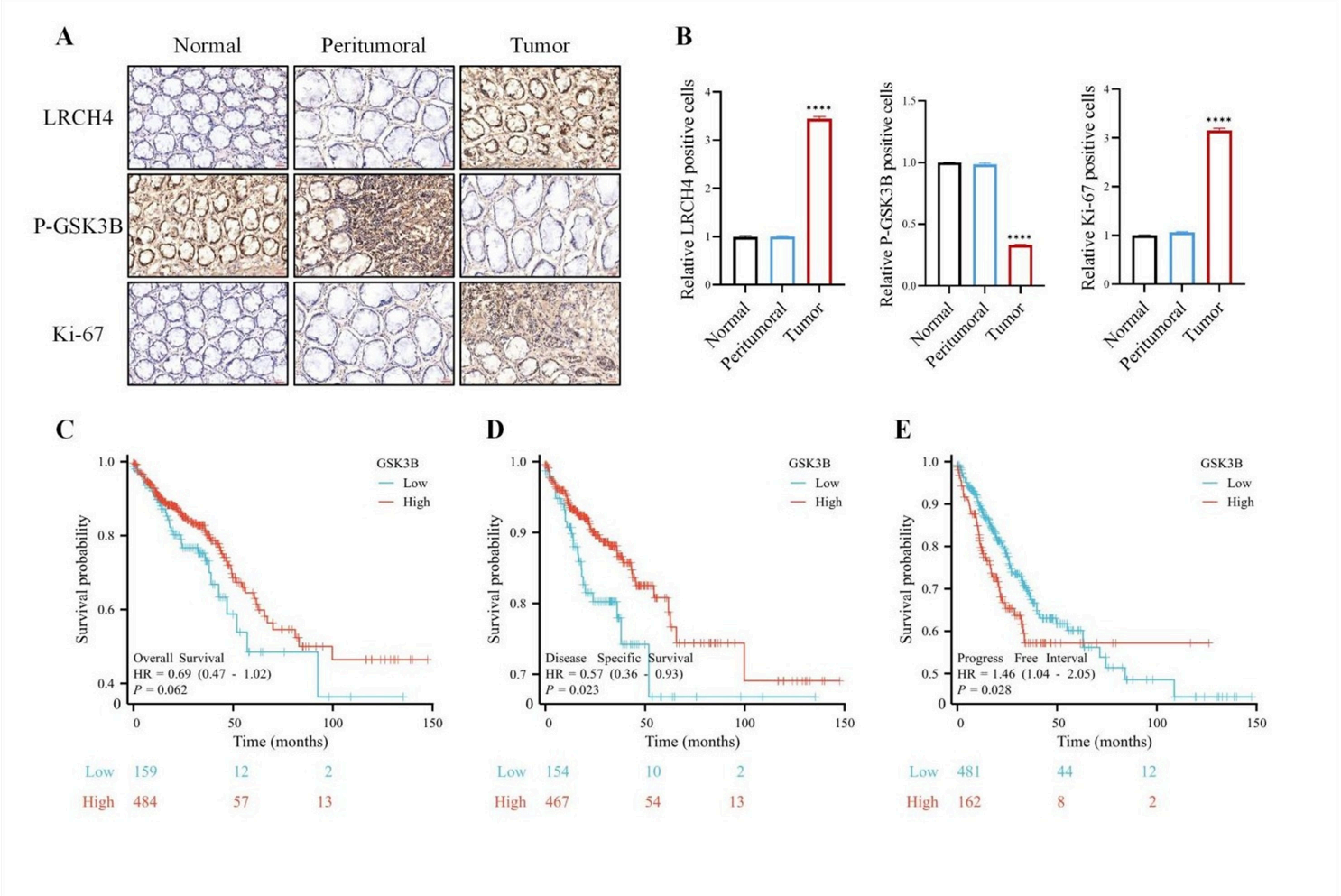


Figure 6

LRCH4 inhibits GSK3B phosphorylation and correlates with poor patient survival. (A, B) Representative immunohistochemical (IHC) staining (A) and quantitative analysis (B) of LRCH4, P-GSK3B, and Ki-67 in normal colon mucosa, adjacent tumor tissues, and primary tumor tissues from CRC patients. Data are presented as mean ± SEM; ****p < 0.0001. (C-E) Kaplan-Meier survival analysis of CRC patients from the KM Plotter database, stratified by low vs. high GSK3B expression. Curves show (C) overall survival (OS), (D) disease-specific survival (DSS), and (E) progression-free survival (PFS). Data from TCGA dataset, and the y-axis minimum was "0".

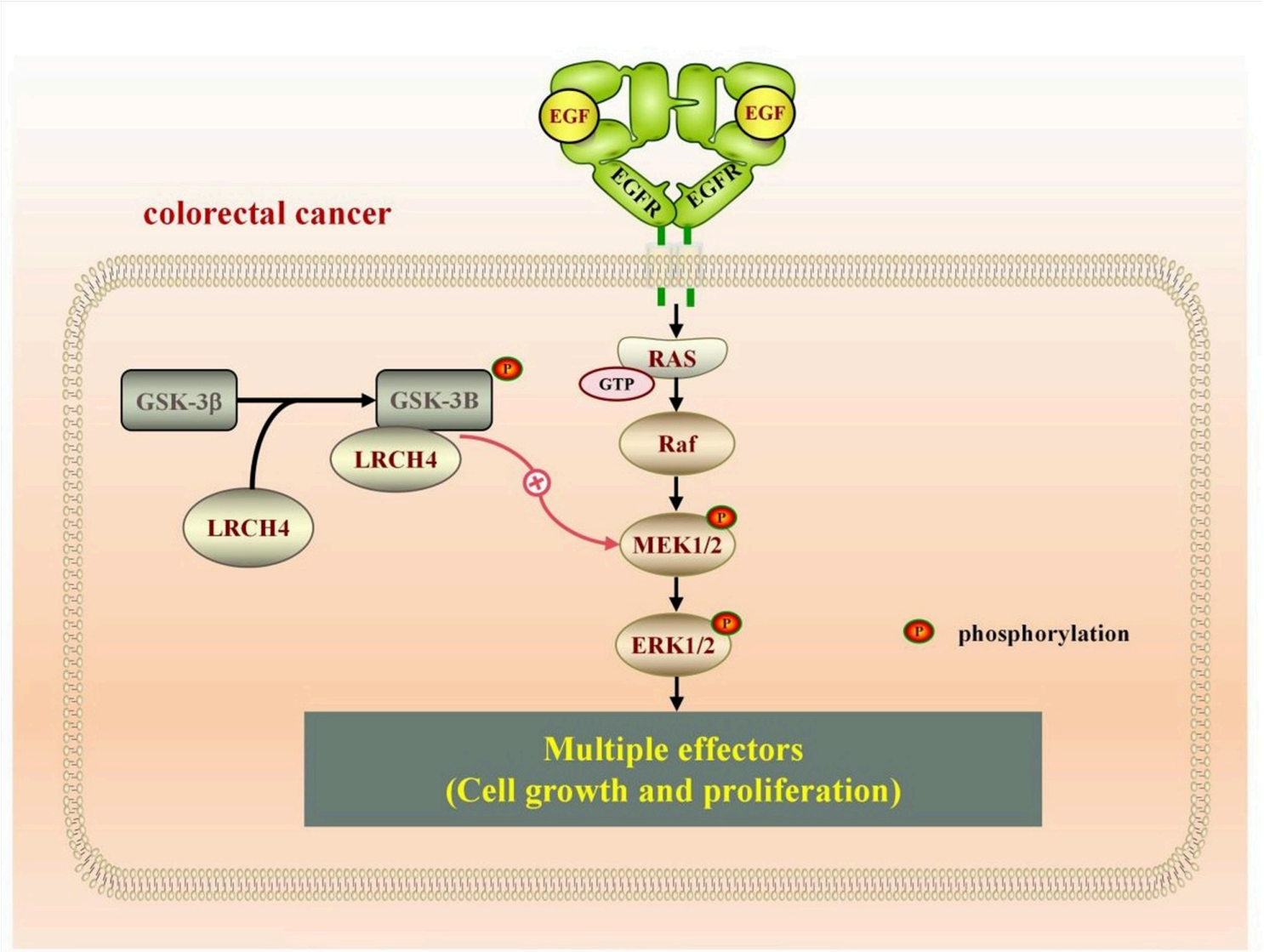


Figure 7

Schematic diagram of LRCH4 driving tumor cell proliferation by regulating the GSK3B/MEK/ERK axis.

Supplementary Files

This is a list of supplementary files associated with this preprint. Click to download.

- originWBfiguresmar.pdf